# Conductor Related Design Considerations for a 1 Meter 10 T $Nb_3Sn$ Dipole Magnet

A. den Ouden, W. A. J. Wessel, H. J. G. Krooshoop, H. van Weeren, H. H. J. ten Kate, G. A. Kirby, R. Ostojic, T. Taylor, and N. Siegel

***Abstract*—A single-bore 1 meter long 10 T $Nb_3Sn$ dipole magnet with a 88 mm bore is being developed. Based on powder-in-tube (PIT) $Nb_3Sn$ strands exhibiting 22 $\mu$m thick filaments, a Rutherford-type cable with a stainless steel core of 25 micron is employed. All properties relevant for magnet design and operation like critical current, filament magnetization and coupling current control have been investigated experimentally. Their impact on magnet operation is discussed. The effectiveness and reliability of a quench protection system for $Nb_3Sn$ accelerator magnets relies mainly on the normal zone propagation properties and properly designed and positioned protection heaters. We present measurements and calculations of propagation properties and discuss the consequences for protection heater design.**

***Index Terms*—Conductor properties, dipole magnet, $Nb_3Sn$, quench protection.**

## I. Introduction

A 1 METER long 2-layer $\cos(\theta)$ 10 T dipole magnet with an 88 mm clear bore utilizing a Powder-in-Tube (PIT) $Nb_3Sn$ conductor is being developed. With this program we aim at the realization of a $Nb_3Sn$ accelerator magnet that closely meets all required accelerator specifications with respect to a field amplitude of 10 T (to be achieved without training), multipole field components in all operation modes below $10^{-4}$, sufficient operating stability and proper quench protection in a self-absorbing mode. General system characteristics and conductor requirements are summarized in Table I [1].

Most of the current $Nb_3Sn$ accelerator magnet programs focus on conductor related issues like enhancement of the critical properties, control of wire manufacturing and cost reduction. Apart from the critical properties also the impact on the field quality of the filament magnetization and optimum values of the crossing and adjacent resistances between the strands in the cable ($R_c$ and $R_a$) are key issues in $Nb_3Sn$ conductor development. Finally, normal zone propagation properties and intrinsic stability of the present high current density $Nb_3Sn$ conductors are intimately related to both conductor and magnet design. Above conductor related issues in the magnet program are being discussed in this paper.

Manuscript received August 5, 2002.

A. den Ouden, W. A. J. Wessel, H. J. G. Krooshoop, H. van Weeren, and H. H. J. ten Kate are with the University of Twente, 7500 AE Enschede, The Netherlands (e-mail: a.denouden@tn.utwente.nl).

G. A. Kirby, R. Ostojic, T. Taylor, and N. Siegel are with CERN, 1211 Geneva, Switzerland (e-mail: g.a.kirby@cern.ch).

Digital Object Identifier 10.1109/TASC.2003.812649

TABLE I
Design Parameters of the 1 meter $\cos(\theta)$ Dipole Model Magnet

| | | |
|---|---|---|
| nominal dipole field @ 4.4 K | 10 | T |
| peak field at pole face | 10.8 | T |
| nominal current | 13 | kA |
| number of coil layers | 2 | |
| clear bore diameter | 87.8 | mm |
| magnetic length | 0.8 | m |
| strand diameter | 0.9 | mm |
| required overall $J_c$ strand @ 10.8 T | 600 | A/mm$^2$ |
| required temperature margin @ 10.8 T | > 1.0 | K |
| copper fraction | ~ 55 | % |
| RRR after heat treatment | >100 | |
| filament diameter | ~22 | μm |
| filament twist pitch | 24 | mm |
| cable dimensions | 16.40x1.79/1.47 | mm |
| number of strands | 35 | |
| stainless steel strip core dimensions | 12.5x0.025 | mm |
| cable twist pitch | 120 | mm |
| cable insulation | folded glass/mica and glass fiber wrap | |
| insulation thickness | 0.14 | mm |

## II. Conductor Properties

### A. Critical Current

An extensive development program has been successfully executed to obtain a well performing stainless steel cored Rutherford-type cable using an adequate PIT-$Nb_3Sn$ conductor that satisfies the demands stated in Table I [1]. The same cable shall be applied for both inner and outer layer coils. The PIT conductors are being developed and manufactured by Shape Metal Innovation, The Netherlands.

Fig. 1 presents the measured noncopper critical current density as a function of the applied field (corrected for self-field) of both a binary $Nb_3Sn$ and ternary $(NbTa)_3Sn$ version of a PIT wire containing 504 filaments with a geometrical $Nb_3Sn$ filament diameter of 22 $\mu$m. Also shown are the properties of the corresponding strands extracted from cored Rutherford cables (Table I). In both cases the permanent current degradation due to cabling is limited to an acceptable amount of $(6 \pm 2)$% at 11 T pointing at only minor filament damage, which is also reflected by a RRR value $>100$ after the heat treatment. Since at present the ternary wire is much more difficult to manufacture we focus in this program on the binary wire.

If strain properties are neglected, proper application of the $J_c(B, T)$ scaling equations for $Nb_3Sn$ conductors [2] shows that at full magnet excitation to 10 T@4.3 K the extracted strand

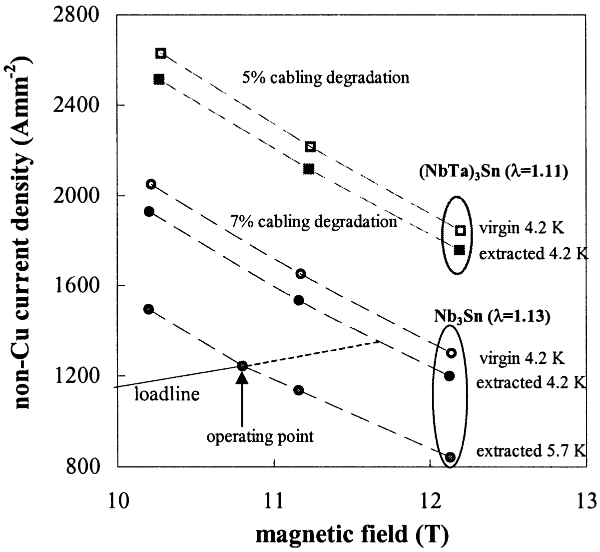


Fig. 1. Non-Cu critical current density of virgin and extracted strands of binary and ternary PIT-504 as a function of the applied magnetic field.

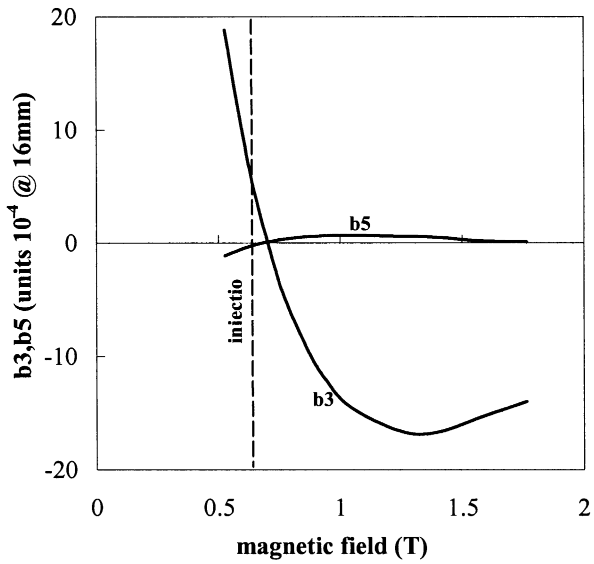


Fig. 2. The normalized sextupole and decapole field components as a function of the central field after a field cycle of 0-3-0.1 T.

has a temperature margin of about 1.4 K at the pole face where the maximum field on the conductor of 10.8 T occurs. Considering that the stress at the pole face is relatively low and that coil manufacturing may also add 5–10% permanent critical current degradation a margin of about 1 K still remains.

However, usually the mid-plane conductors (10.1 T at full magnet excitation) experience the maximum radiation heat load and the maximum transverse stress (~130 MPa) at full excitation. Additional to the manufacturing margin the stress introduces a nonpermanent $I_c$ reduction of 5–10%. In this view the margin in current density for the mid-plane conductors of about 30% (corresponding temperature is 6.6 K) is probably adequate but not excessive.

### *B. Filament Magnetization*

Experimental magnetization data of both binary and ternary PIT-504 $Nb_3Sn$ wires have been reported earlier [1]. These experimental data have been used in a simulation program to calculate the impact of the filament magnetization on the field harmonics at low fields [3] using a yoke configuration that had been configured separately to ensure a low and at all stages flat multipole field content. In the simulation a conditioning cycle 0-3–0.1 T precedes the final ramp to injection and full coil excitation. Fig. 2 shows the resulting sextupole and decapole field components in units $10^{-4}$ at a reference radius of 16 mm. At injection the sextupole is about $+7.5$ units while during the up-ramp a minimum of $-17$ units occurs at a relatively high field of 1.3 T. The decapole is within the aimed range. Though this is a remarkable improvement compared to the 11 T dipole magnet MSUT for which a PIT conductor with 55 $\mu$m filaments was employed, the aimed level close to 1 unit is not achieved yet.

Further reduction of the sextupole component can be accomplished in two ways. One approach is a re-optimization of the detailed shape of the iron yoke that enables preferentially reshaping of the sextupole or the decapole some tenths of units in this field range. Another attractive way of multipole compensation is insertion of iron strips along the coils at properly chosen positions before collaring or eventually on a beam screen after magnet assembly [4]. Both options shall be investigated before the final magnet assembly.

### *C. Coupling Current Control*

Coil manufacturing and heat treatment of the wound coils will follow tightly the procedures as they were employed for the 11 T MSUT dipole magnet. In this magnet unacceptable large dynamic field components of tenths of units during current ramping have been observed. They were generated by large coupling currents, mainly as a result of low values (~1 $\mu\Omega$) of both the adjacent strand resistance $R_a$ and the crossing strand resistance $R_c$ [5]. Control of these resistances is a compromise between current sharing capabilities (low values), suppression of coupling currents (high values) and thermal stability (low values). Insertion of a 25–50 $\mu$m thick and 12.5 mm wide stainless steel strip between the strand layers (covering about 3/4 of the cable width) may offer an acceptable compromise to realize an increase of $R_c$ to 15–50 $\mu\Omega$ while maintaining a preferred low $R_a$ of a few $\mu\Omega$. However, the obtained values after core insertion strongly depend on, for instance, the heat treatment (stress, temperature, cable cleaning), the overall compaction of the cable and the surface conditions of the strands. Therefore it is strongly advised to measure $R_a$ and $R_c$ for each particular cable.

$R_a$ and $R_c$ are extracted from calorimetric loss measurements on a stack of 6 cables each 3 twist pitches long. Sample preparation follows closely the coil manufacturing conditions with respect to effective size, pressure, heat treatment and resin impregnation. After applying a transverse load of about 30 MPa the stack is exposed at 4.3 K to a sinusoidal swept dipole field with an amplitude of 300 mT up to a frequency of 250 mHz oriented both perpendicular and parallel to the wide side of the cable. Since the inter-filament loss component can be estimated fairly accurate from the RRR value of 100, the Cu ratio $\lambda$ and the filament twist pitch of 22 mm, the loss contributions from

$R_a$ and $R_c$ can be derived from the $(Q, f)$ results, with $Q$ the loss in kJm$^{-3}$ per field cycle [6].

The obtained values are respectively: $R_a = (10 \pm 3)\ \mu\Omega$ and $R_c = (60 \pm 15)\ \mu\Omega$. Compared to reported $R_c$-values of differently treated cored $Nb_3Sn$ cables ranging from 30 to 80 $\mu\Omega$ this $R_c$ value fits well in this window and is close enough to the aimed range [6].

### *D. Normal Zone Propagation*

To study and design a quench protection system knowledge about the normal zone propagation (NZP) properties of the conductor in a representative $(I, B, T)$ range is mandatory. Since these have never been investigated either experimentally or theoretically for PIT-$Nb_3Sn$ conductors we have developed a facility to measure near adiabatic normal zone properties in vacuum. At a presently lowest temperature of (4.8.0 ± 0.1) K, in fields up to 12 T and for currents up to 500 A the set-up enables measurement of NZP properties of helical samples with a length of 1 meter with complete control of the cooling conditions. NZP velocities are measured by the voltage time-of-flight method after applying a millisecond range heat pulse with a wire wound heater. $Nb_3Sn$ samples are heat treated on a standard TiAlV barrel, transferred to the cotton-phenolic (C-P) measuring sample holder and finally soldered to the current leads.

After the NZP measurements at 4.8 K, LHe is allowed into the vacuum chamber to enable a proper $I_c$ measurement at 4.25 K in field. Again, by applying the scaling equations for $I_c\,(B, T)$ the critical parameters at 4.8 K at the very same strain conditions of the particular sample are obtained with an accuracy of about 2%. The difference in thermal contraction of 0.12% between the standard TiAlV sample holder for $I_c$ measurements and the C-P sample holder for NZP measurements is used to correct for the strain difference of the $Nb_3Sn$. The resulting $I_c$ (C-P) agrees within a few percent with the independently measured $I_c$ on the C-P sample holder.

In parallel to the experiments a quasi-3D fully explicit finite difference numerical model is developed to simulate both the longitudinal and turn-to-turn normal zone propagation under adiabatic conditions as well as the protection heater characteristics. Where applicable material properties are considered temperature and field dependent.

Fig. 3 shows the experimental and simulated normal zone propagation velocity as a function of the normalized transport current $(I/I_c\,(B, T))$ of a binary PIT-504 wire in background fields of 11 and 12 T @ 4.8 K. Measured values are accurate within 7%. By adjusting only the heat capacity of the unknown residuals of the powder core in the filaments to reasonable values, satisfactory agreement between measurements and simulations is obtained, especially at higher velocities where nonperfect adiabatic conditions become relatively less important. These results justify applicability of the numerical scheme to a much wider $B$, $T$, $I$-range.

The relatively low longitudinal NZP velocities are comparable to those measured on the MSUT dipole magnet. This is also the case for the turn-to-turn delay values in the range of 5–50 ms at 11 T over the current range of interest [5].

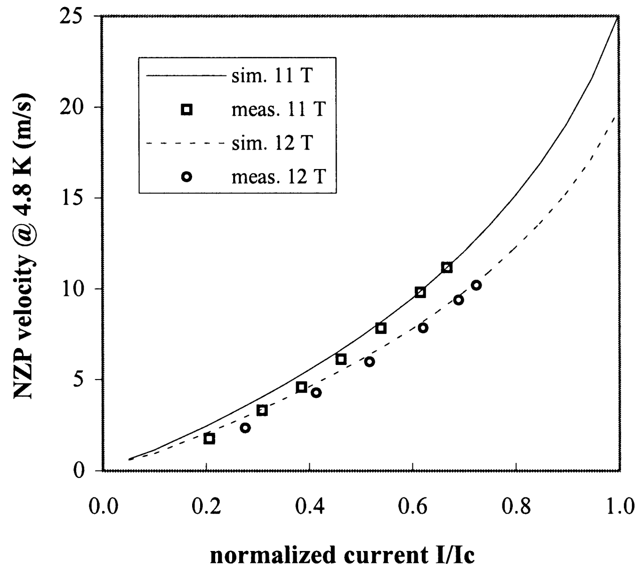


Fig. 3. Normal zone propagation velocity of a binary PIT-504 $Nb_3Sn$ conductor (see Table I) at 4.8 K in a background field of 11 and 12 T respectively. Also shown are the results from numerical simulations under adiabatic conditions.

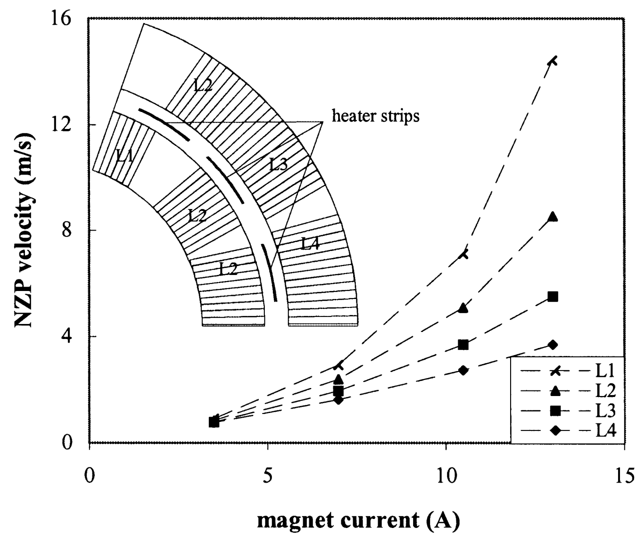


Fig. 4. Simulated NZP velocities as a function of the magnet current at conductors sites in the coils depicted in the schematic coil cross section. Also shown are the proposed locations of the quench heaters.

## III. Protection Heaters

Quench protection of accelerator magnets depends mainly on the effectiveness of the protection heater system. We intend to follow the approach of the protection system for the LHC dipole magnets by using stainless steel strip heaters that are periodically covered with a copper cladding to reduce the active resistive area without losing effectiveness [7]. Positioning of the heaters, ratio and periodicity of the copper cladding, width of the strips and the required power density are mainly determined by the coil layout [local $T_c(I_c(B))$ as function of the current], properties of the cable insulation, coil manufacturing procedures and the normal zone propagation (NZP) properties of the conductor.

Using the numerical scheme above NZP velocities in the coils as a function of the magnet current are calculated. Fig. 4 shows the results at several locations in the coil cross-section.

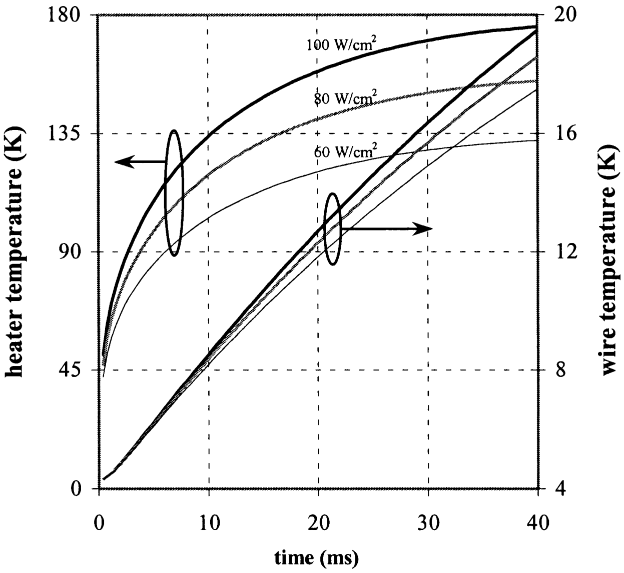


Fig. 5. Time dependence of the heater temperature and conductor temperature at several heater power densities. The time constant for the heater current is 52 ms.

It should be noted that despite the large field gradients in the conductors the average field appears to be a fair value for the NZP properties. As a result of the comfortable but necessary $(T_c, I_c)$-margin the NZP velocities are correspondingly low. Apart from the pole face conductor block (L1 in Fig. 4) the velocity remains below 10 m/s at full magnet excitation. The $(T_c, I_c)$-margin also implies relatively high current sharing temperatures $T_{cs}$ at which heat generation starts during the transition to the normal state. For the conductors covered by the quench heaters (Fig. 4) $T_{cs}$ ranges from 7 to 14 K at full excitation. This imposes a smaller longitudinal periodicity of the copper cladding on the heater strips and probably demands more power than typical LHC protection heaters.

The proposed quench heaters in Fig. 4 (covering about 70% of all conductors) consist of a 25 $\mu$m thick, 15 mm wide stainless steel strip, covered on both sides with glue (22 $\mu$m), Kapton (75 $\mu$m) and glass fiber (50 $\mu$m) and are impregnated with the coils. For heater power densities ranging from 60–100 Wcm$^{-2}$ the temperature evolution of the covered part of the underlying conductor (~6 mm) is depicted in Fig. 5. An important conclusion from these calculations is that with moderate heater power density all conductors can be brought into transition within 40 ms, which at present is considered adequate for protection purposes.

Above results supply all necessary input to design a quench protection system not only for this model magnet but also for a full-size (~10 meter long) magnet. This shall be carried out in the next design stage.

## IV. Conclusions

A 10 T $Nb_3Sn$ model magnet utilizing a successfully developed binary PIT-based Rutherford-type cable is being developed. Relevant conductor properties with respect to critical current, magnetization, stress sensitivity, interstrand resistance and NZP of samples from the realized conductor have been investigated experimentally.

At full magnet operation the required margins in the critical parameters $I_c$ and $T_c$, which should allow for radiation heat absorption may conflict with quench protection requirements. Though the proposed quench heaters enable fast heat transfer to the coils this issue demands detailed investigation of the quench process of the whole magnet.

## Acknowledgment

The authors would like to thank Christine Voellinger and Stephan Russenschuck of CERN for performing the field calculations incorporating the filament magnetization and our colleagues at LBNL for fabricating the cored Rutherford cables. We highly appreciate the skills and dedication of the people at ShapeMetal Innovation for their ongoing work on PIT-$Nb_3Sn$ conductor development and manufacturing.

## References

[1] A. den Ouden *et al.*, "Progress in the development of an 88 mm bore 10 T $Nb_3Sn$ dipole magnet," *IEEE Trans. on Applied Superconductivity*, vol. 11, no. 1, pp. 2268–2271, 2001.

[2] A. Godeke, B. ten Haken, and H. H. J. ten Kate, "Scaling of the critical current in ITER type $Nb_3Sn$ conductors in relation to applied field, temperature and uni-axial strain," *IEEE Trans. on Applied Superconductivity*, vol. 9, no. 2, pp. 161–164, 1999.

[3] M. Aleksa, S. Russenschuck, and C. Voellinger, "Magnetic field calculations including the impact of persistent currents in superconducting filaments," *IEEE Trans on Magnetcs*, vol. 38, no. 2, pp. 825–828, 2002.

[4] V. V. Kashikin and A. V. Zlobin, "Correction of persistent current effect in $Nb_3Sn$ dipole magnets," *IEEE Trans. on Applied Superconductivity*, vol. 11, no. 1, pp. 2058–2062, 2001.

[5] A. den Ouden *et al.*, "Quench characteristics of the 11 T $Nb_3Sn$ dipole magnet MSUT," in *Proceedings of the 15th International Conference on Magnet Technology*, Beijing, 1997, pp. 137–141.

[6] M. D. Sumption, E. W. Collings, R. M. Scalan, A. Nijhuis, and H. H. J. ten Kate, "Core suppressed AC loss and strand-moderated contact resistance in a $Nb_3Sn$ Rutherford cable," *Cryogenics*, vol. 39, pp. 1–12, 1999.

[7] F. Rodriguez-Mateos and F. Sonneman, "Quench heater studies for the LHC magnets," in *Proceedings of the 2001 Particle Accelerator Conference*, Chicago, USA, pp. 3451–3453.